Chinese Journal of Physiology 56(1): 52-57, 2013
DOI: 10.4077/CJP.2013.BAA072

Determination of Glottic Opening Fluctuation by a New Method Based on Nasopharyngoscopy

Yuanyuan Chen[1], Geoffrey Maksym[2], Timothy Brown[3], and Linhong Deng[1, 4]

[1]*Key Laboratory of Biorheological Science and Technology, Ministry of Education, College of Bioengineering, Chongqing University, Chongqing 400044, People's Republic of China*
[2]*School of Biomedical Engineering, Dalhousie University, Halifax, Nova Scotia, Canada B3J 3H5*
[3]*Division of Otolaryngology, Department of Surgery, Dalhousie University, Halifax, Nova Scotia, Canada, B3H 1V7*
and
[4]*Institute of Biomedical Engineering and Health Sciences, Changzhou University, Changzhou 213164, Jiangsu, People's Republic of China*

Abstract

Understanding the opening fluctuation of glottis is meaningful in diagnosing vocal cord dysfunction. Nasopharyngoscopy can offer a direct method for visualizing the opening and closing of the glottis. However, the large amount of image data presents a significant challenge for quantitative analysis of the video recordings. Thus, automatic image processing method allowing for batch analysis of glottic images becomes clinically important. Here, we present an image processing method using Gaussian smoothing filter and threshold segmentation, followed by differentiation and Canny image edge detection for tracking changes in glottis dimensions (the opening area). A quantitative assessment of true glottic size was also developed for calibration in our study. This method was used to analyze different video data acquired from clinical nasopharyngoscopy of 8 healthy subjects during either normal breathing, breathing with cough or with 'Hee' sound. The results indicated that the computed glottic area change waveform was consistent with the observed glottic fluctuation in the video from nasopharyngoscopy. Thus, our proposed method may provide an accurate and efficient detection of glottic aperture and quick assessment of glottic fluctuations to assist clinical diagnosis of vocal cord dysfunction and other airway pathologies.

Key Words: glottis, nasopharyngoscope, vocal fold, vocal fold dysfunction, breathing, cough

Introduction

The larynx is the primary organ for phonation, that is, the generation of glottal tone. To understand how glottal tone is influenced in health and disease, researchers have studied glottal behavior for nearly a century. Directly visualizing the vocal cords can be helpful in the diagnosis of pulmonary disorders, particularly the vocal cord dysfunction (VCD) (10, 11). VCD is the intermittent and abnormal adduction of the vocal cords during respiration. Common symptoms of VCD include intermittent shortness of breath, wheezing, stridor and cough, which may be interpreted as worsening asthma, subglottic stenosis, tracheal masses and laryngeal edema.

The standard criterion for diagnosing VCD is by direct observation of vocal cords during inspiration while the patient has symptoms (3). This is usually done by using flexible fiberoptic nasopharyngoscopy to video image the glottic space (10). It can be per-

Corresponding author: Linhong Deng, Ph.D., Professor & Director of Key Laboratory of Biorheological Science and Technology, Ministry of Education, College of Bioengineering, Chongqing University, Chongqing 400044, People's Republic of China. E-mail: denglh@cqu.edu.cn
Received: September 28, 2011; Revised: December 13, 2011; Accepted: March 23, 2012.

Table 1. Demographics of the test subjects (mean ± STD)

Age (year)	Gender (Male : Female)	Height (cm)	Weight (kg)
33.63 ± 13.98	5:3	171.38 ± 7.38	69.75 ± 7.55

formed painlessly and slowly, which allows for excellent visualization, without gagging, of the entire upper airways from the nares to the vocal cords. Therefore, it has become a common procedure with minimal morbidity (19). However, to our knowledge, quantitative analysis of glottic fluctuations by nasopharyngoscopy in human subjects has not been reported, likely due to the difficulty in analyzing the large amount of the video image data.

In order to develop a method to automatically detect the intermittent adduction of vocal cords, a method of image analysis was proposed in this paper, which included an automatic algorithm developed on Matlab® (The MathWorks Inc., Nortic, MA, USA). Using this method, we analyzed the glottal area changes of 8 healthy human subjects during either normal breathing, breathing with cough or with 'Hee' sound. We demonstrate that this method can detect not only the slow changes during normal breathing, but also the abrupt changes during coughing and sound-making, the latter is especially important as it has not been detected using other video processing methods. These data suggest that our method can determine the glottic fluctuation efficiently and effectively which will be meaningful to diagnosis of airway diseases such as VCD.

Materials and Methods

Subjects

Eight healthy human subjects were recruited for this study. They were between 16 to 70 years old, without history of smoking. In addition, none of them was associated with history of VCD or other chronic respiratory or upper airway conditions or recent respiratory tract infection. The demographics of the subjects are presented in Table 1. All protocols used in this study including proper informed consent of subject had been approved by the Institutional Review Board (Capital Health Research Ethics Board) of Dalhousie University, Canada.

Video Data Collection

A nasopharyngoscope (Olympus Exera CLV-180, Tokyo, Japan) was used to visualize the movements of the glottis aperture. The tip of the scope was coupled to a charge coupled device (CCD) camera working in the red-green-blue (RGB) color system. The signals from the camera were displayed in real time on the monitor while appropriate sequences were recorded on the computer. Before beginning the procedure, the subject was given a thorough explanation of what was to be done, indications for the procedure, and any alternatives, if they existed (6, 19). The subject was placed in a sitting and slightly reclined sitting position for comfort. Prior to insertion of the nasopharyngoscope, topical anesthetic (xylocaine spray 10%) was administered to the nostrils +/– topical decongestant, Otrivin® (Novartis Inc., Mississauga, ON, Canada) depending on whether the subjects could tolerate the presence of the scope. After anesthesia, the scope was carefully inserted until the vocal cords were in view, while the scope was kept away from the pharyngeal walls as far as possible. All nasopharyngoscopy procedures for collecting video data were performed by the same physician (Dr. Timothy Brown).

Recording was not initiated until the breathing pattern had stabilized and the respiratory movements of the glottis appeared to be reproducible. In all measurements two different sessions were included, *i.e.* one minute recording during normal breathing, followed by another one minute recording during normal breathing with a single cough and 'Hee' sound for about 5 sec at the given time points. The single cough and ~5 sec of "Hee" sound made by the subject during normal breathing were required to induce the abrupt change of the throat and glottis, and the short-period closure of the glottis, respectively.

Image Processing Method

In order to process the video images efficiently, the recorded RGB images were first converted to gray images. Subsequently, the gray images were processed by using the custom developed image processing method for tracking the changing glottis dimensions as shown in Fig. 1. The method combined several techniques including Gaussian smoothing filter, threshold segmentation, differentiation, and Canny image edge detection in order to accomplish effective detection of the moving glottis edge, which was not possible by the classical edge detection method (5, 15, 20). The algorithm was developed in the Matlab® software and executed using an Intel® Pentium® 4 CPU 2.8 GHz processor. More details about this method were described in the following.

Smoothing is an image processing technique

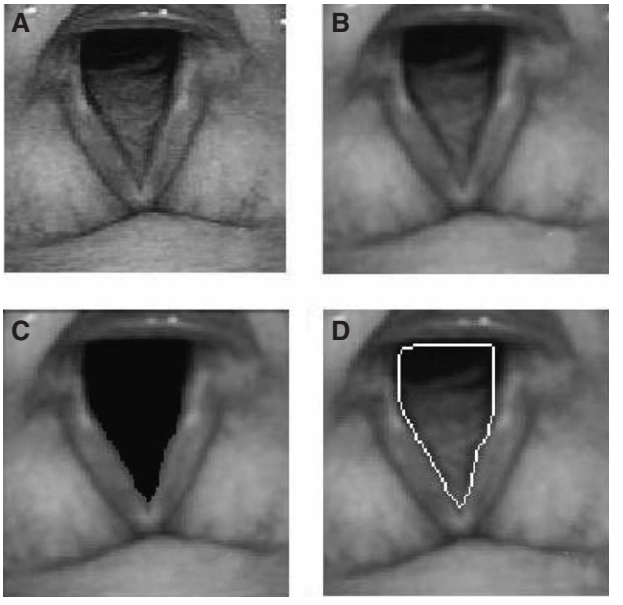

Fig. 1. Nasopharyngoscopically-captured video image of the glottis before and after being processed by the custom developed image analysis method. (A) A single frame of the video image before imaging processing; (B) the same frame of the video image after being smoothed by the Gaussian smoothing filter; (C) after threshold segmentation and differentiation; (D) after the Canny edge detection to detect the glottis edge as traced by the white line.

that averages the image data points with their neighbors in the image. The primary reason for smoothing is to increase the signal to noise ratio. Smoothing is also referred to as filtering, because it has the effects of suppressing high frequency signal and enhancing low frequency signals. In this study, the image was smoothed by a Gaussian smoothing filter that was a linear convolution filter based on a filter kernel that was convoluted with an image. The Gaussian width was specified either with qualifier sigma or as a default value of 1.5 pixels. The filter kernel itself was considered and viewed as either an image in two dimensions (2D) or a curve in one dimension (1D).

Below are the formulas for 1D and 2D Gaussian filter where SDx and SDy are the standard deviation for the x and y directions, respectively.

$$K_{1D} = e^{\frac{-i^2}{2 \cdot SD^2}} \tag{1}$$

$$K_{2D} = e^{\frac{-i^2}{2 \cdot SDx^2}} e^{\frac{-j^2}{2 \cdot SDy^2}} \tag{2}$$

The glottal edge was usually represented by the points of greatest change in the image intensity corresponding to the extreme values of the image intensity (21). Once the image was smoothed, the glottal area was determined by using the fixed threshold segmentation technique (Fig. 1B). The fixed threshold segmentation technique used fixed threshold to divide pixels into two areas, those with the intensity values greater than the threshold were kept unchanged but those with intensity values less than threshold were all reset as zero for their intensity values, The recorded image displayed the glottal opening as an almost pitch black area, with which a threshold of 20 (sometimes 25 or 30, depending on the brightness of the video) could turn the glottal area uniformly black. Thus the differentiation was larger than beforehand. Then the horizontal differentiation along the pixel rows of the image was used to determine the extreme values of the image intensity below the black area. The minimal and maximal values gave the left and right boundaries of the vocal folds in the image (Fig. 1C).

In the final step, Canny edge detection (5) was used to obtain a continuous glottal edge. Canny edge detection is a double threshold algorithm, thus a low threshold and high threshold were applied to obtain edge in an image. If the gradient of a pixel was above the high threshold, there was a clear edge at that point and it was therefore described as an edge pixel. Otherwise, if the gradient of the pixel was below the low threshold, the edge at this point was very faint and thus was declared as a non-edge pixel. The pixel with gradient in between can be declared as an edge pixel only if it was connected to a definite edge pixel either directly or *via* other pixels with gradients between the low and high thresholds (5, 21).

Nasopharyngoscope Calibration

Quantitative assessment of glottis aperture was also developed as follows. In order to obtain the true glottic size from the video, the nasopharyngoscope was calibrated to determine the relationship of distance between the CCD camera and the equivalent pixels of an object with known size, in this case a 1 cm scale on a ruler. A conversion factor (CF) from pixels to centimeters was calculated on the calibration grid at different distances (d) from the scope tip. A nonlinear function between CF and d was obtained (R Square = 0.998) as shown in Fig. 2B. The calibration curve was further tested for its accuracy by using the nasopharyngoscope to take pictures of a coin (diameter = 24.02 mm) at 3 different distances. The mean diameter of the coin calculated with the above function turned out to be 23.68 mm, which represented an approximate accuracy of 98.59%.

The above calibration demonstrated that the distance between the glottis and the tip of the scope was critical to the accuracy of the image based mea-

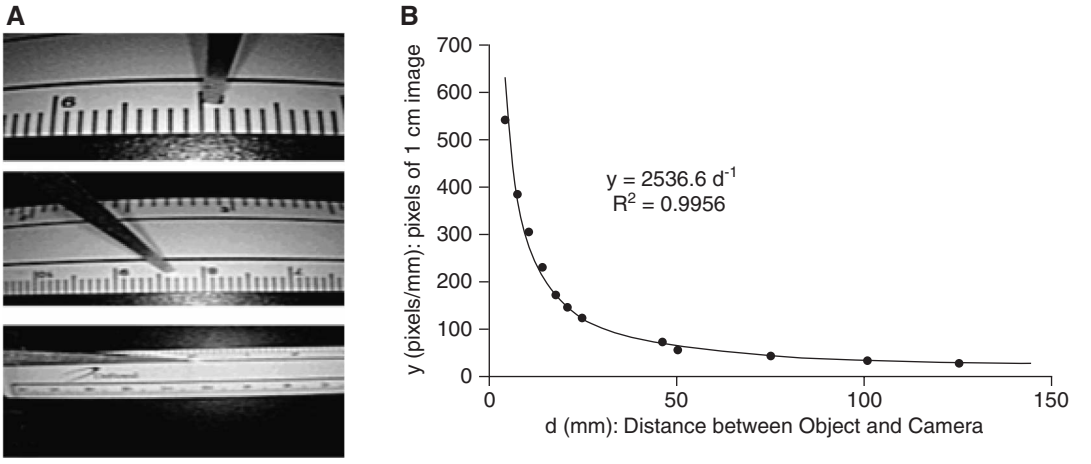

Fig. 2. Calibration of the nasopharyngoscope for measuring the glottis size. (A) A ruler was fixed on the desk and the nasopharyngoscope was used to take pictures of the ruler while the tip of the scope was held vertically above the ruler at different distances (d); (B) For each image taken at a given distance (d), a conversion factor between the number of image pixels to the real dimension of the object, *i.e.* the actual scale on the ruler was obtained, and relationship between the conversion factor and the distance, d could be established if this calibration procedure was done for sufficient number of distances. A nonlinear function was thus established for calculating the glottis size for a recorded image taken at a known distance.

surement of glottis size. However, in the nasopharyngoscopy the actual distance between the tip of the scope and the glottis could not be measured directly. Therefore, we took images of the glottis at two (or more) different distances and the relative distances between images taken were recorded. This distance was computed on the assumption that the subject did not vary his/her gesture between the different phases of measurement. In our experiment, we took pictures of glottis in 3 different positions, and used the mean value of the distance as the distance between the glottis and the tip of the scope. Thus the true glottis size could be calculated using the above calibration function in Fig. 2B.

Results

A representative example of glottis images of one subject's glottis images as captured from the video at different time points in different breathing stages is shown in Fig. 3. The video clearly shows that the aperture of the laryngeal glottis narrowed on expiration (Fig. 3A) and widened on inspiration (Fig. 3B) during quiet breathing. The widening generally commenced before the onset of inspiration, whereas the narrowing preceded the onset of expiration. From our observation, the glottis width was greater on inspiration than on expiration in the whole measurement and did not show any disorder. When the subject was asked to cough, the glottis almost closed immediately (Fig. 3C), then began returning to open for normal breathing. The closure induced by cough just lasted a short time, and was less tight as compared to that induced by the subject's making the 'Hee' sound, as we observed.

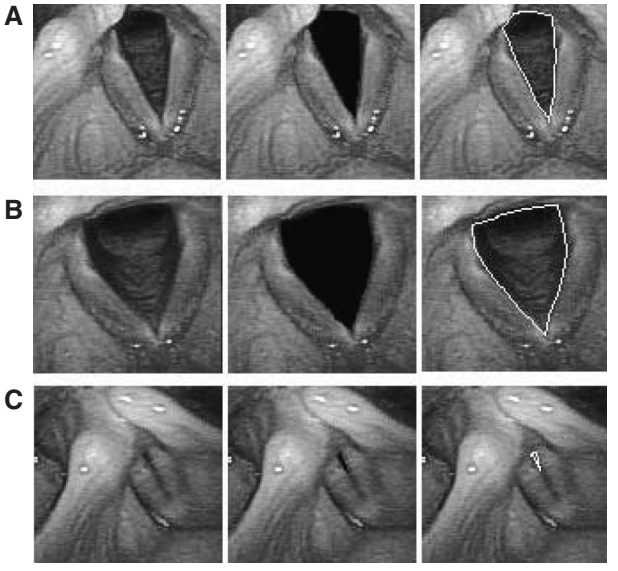

Fig. 3. Changing shapes of the glottis during different respiratory maneuvers and the corresponding glottis edges detected by the image processing method. From left to right are glottis images before processing, after processing, and with edge detected as indicated by the white trace line in the image. Panels A and B display images of the glottis during expiration and inspiration, respectively. Panel C displays images of closed glottis during coughing or making 'Hee' sound.

Fig. 4 displays the glottal area (Ag) change wave of a typical subject during either breathing with

Table 2. The measured glottal area of each individual subject during inspiration (max), expiration (min) and the group average (mean) (cm^2)

Subject	1	2	3	4	5	6	7	8	Means ± STD
Max (cm^2)	0.65	0.81	0.93	1.35	1.34	0.71	1.27	0.77	0.98 ± 0.29
Min (cm^2)	0.43	0.61	0.68	1.15	0.11	0.54	0.95	0.58	0.76 ± 0.28

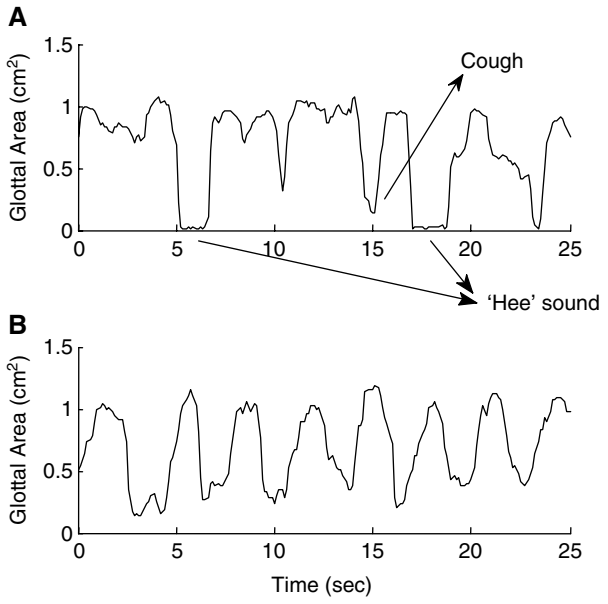

Fig. 4. Change wave of glottal area extracted from the video images by the image processing method. (A) The change wave of glottal area during normal breathing with cough and "Hee" sound maneuvers; (B) the change wave of glottal area during normal breathing only.

cough and 'Hee' sound (Fig. 4A) or quiet breathing (Fig. 4B), as quantitatively assessed by the image processing method. It can be seen that during normal breathing the glottis area change wave went up and down with time. The crest and the trough of the wave corresponded to the inspiration and expiration, respectively. When subject coughed, the glottis area jumped to almost zero. In comparison, when the subject made the 'Hee' sound, the glottis area not only decreased to almost zero but also kept the closure state for a few seconds.

Table 2 gives the results of measurement of maximal, minimal, and the averaged glottal area during inspiration and expiration, respectively, for the 8 human subjects. The data show fairly large variations of the glottis area between individual subjects. However, the opening of the glottis from expiration to inspiration was consistent among all the subjects as indicated by the consistent increase of glottis area for each individual subject and the averaged above 20% increase of glottis area for the whole group.

Discussion

The main purpose of this study was to develop a video processing method for automatic determination of fluctuation of glottis movements. The method we described in this report took advantage of various image processing techniques, and was capable of batch analysis of large amount of image data collected from clinical nasopharyngoscopy. Using this method, we were able to generate highly reproducible and accurate change wave of the glottis area of an individual subject during different breathing patterns such as normal quiet breathing, breathing with cough or making "Hee" sound for mimicking speaking. The results demonstrated that the change waves corresponded well to the glottis fluctuations as observed in the video. However, the change wave could not only show the glottis movements more directly, but also detected abnormal behavior of the glottis more effectively, as compared with the manual frame-by-frame detection.

To our knowledge, there has been no previous report on using nasopharyngoscope to visualize and quantitatively assess the respiratory movements. Some researchers have previously examined respiratory movements of the vocal cords in human subjects. For example, Rattenborg (16) examined respiratory movements using indirect techniques in the early 1961. Jackson *et al.* (13) used a video system to examine glottic aperture during panting. England *et al.* (9) reported measurements of changes in glottic width during quiet breathing. All these studies were similar to our present study, but they neither quantified the glottic dimensions and nor included the cough and 'Hee' sound making in their study.

The glottis may close or change abruptly because of episodic swallowing and speaking. For the purpose of determining the glottic aperture change over these periods, the subjects were asked to cough and make 'Hee' sound during the measurements. There were obvious glottal area fluctuations which synchronized with the glottis sudden movements. Our observation showed that the aperture of the laryngeal glottis widened on inspiration and narrowed on expiration during quiet breathing. This is in agreement with the study of Baier *et al.* (2), and Brancatisano *et al.* (4).

The accuracy of measurement of the glottis size

is largely dependent on the distance between the glottis and the tip of the scope. The main source of error comes from the resolution of the tool measuring the distance and reliability of the operator who take the measurement. However, there are other sources of error which remain less understood and hard to deal with including the angle between the glottis and the nasopharyngoscope (7). In our study, this angle was assumed to be 90 degrees. Hanson *et al*. (12), using a rigid endoscope, estimated that the amount of tilt of the larynx is less than 10 degrees. It should be noted that the tilt angle is difficult to visualize clearly and estimate accurately, which could contribute additional error to the measurement. Previous studies (1, 8, 14) have attempted to correct the images for the tilt effect by using numerical method and correction algorithms, but it is hard to develop a universal correction algorithm for different kinds of scope. Therefore, for further improving the measurement, one may need to solve the effect of tilt by new scope designs that make it possible to determine the distance between glottis and the tip of the scope both easily and accurately (7, 18).

On the other hand, the results obtained by the present method were consistent with the literature. For example, the average glottis area that we obtained from measuring 8 healthy human subjects was about 0.98 cm^2, which agrees with Rigau's calculation (17). The measurement was highly reproducible for a given individual but there were still large variations (~30%) between individual subjects. These large variations may partly due to the small sample size (n = 8) for this study, which should be further validated with larger group of subjects in future study. Nevertheless, this preliminary study with limited sample size at least provide a proof of concept for using nasopharyngoscopic images to detect and assess the respiratory movement of glottis, and ultimately help clinical practice for diagnosis and treatment of upper airway conditions such as VCD.

In conclusion, we have proposed an image processing algorithm that can detect and quantify not only the glottis fluctuations during normal quiet breathing, but also the abrupt changes of glottis fluctuations during active respiratory events such as coughing and speaking. Our results provide for the first time direct evidence that such measurement is possible. And if this technique is further validated in future studies, it may provide a valuable tool for biomedical research and clinical applications of laryngeal physiology and pathology.

Reference

1. Asari, K.V., Kumar, S. and Radhakrishnan, D. Technique of distortion correction in endoscopic images using a polynomial expansion. *Med. Biol. Eng. Comput*. 37: 8-12, 1999.
2. Baier, H., Wanner, A., Zarzecki, S. and Sackner, M.A. Relationships among glottis opening, respiratory flow, and upper airway resistance in humans. *J. Appl. Physiol*. 43: 603-611, 1977.
3. Benninger, C., Parsons, J.P. and Mastronarde, J.G. Vocal cord dysfunction and asthma. *Curr. Opin. Pulm. Med*. 17: 45-49, 2011.
4. Brancatisano, T., Collett, P.W. and Engel, L.A. Respiratory movements of the vocal cords. *J. Appl. Physiol*. 54: 1269-1276, 1983.
5. Canny, J. A Computational Approach to Edge-Detection. *IEEE Trans. Pattern Anal. Mach. Intell*. 8: 679-698, 1986.
6. Czaja, P., Soja, J., Grzanka, P., Cmiel, A., Szczeklik, A. and Sladek, K. Assessment of airway caliber in quantitative videobronchoscopy. *Respiration* 74: 432-438, 2007.
7. Dailey, S.H., Kobler, J.B., Hillman, R.E., Tangrom, K., Thananart, E., Mauri, M. and Zeitels, S.M. Endoscopic measurement of vocal fold movement during adduction and abduction. *Laryngoscope* 115: 178-183, 2005.
8. Dorffel, W.V., Fietze, I., Hentschel, D., Liebetruth, J., Ruckert, Y., Rogalla, P., Wernecke, K.D., Baumann, G. and Witt, C. A new bronchoscopic method to measure airway size. *Eur. Respir. J*. 14: 783-788, 1999.
9. England, S.J., Bartlett, D. and Daubenspeck, J.A. Influence of human vocal cord movements on airflow and resistance during eupnea. *J. Appl. Physiol*. 52: 773-779, 1982.
10. Gimenez, L.M. and Zafra, H. Vocal cord dysfunction: an update. *Ann. Allergy Asthma Immunol*. 106: 267-274, 2011.
11. Greenberger, P.A. and Grammer, L.C. Pulmonary disorders, including vocal cord dysfunction. *J. Allergy Clin. Immunol*. 125: S248-S254, 2010.
12. Hanson, D.G., Jiang, J., D'Agostino, M. and Herzon, G. Clinical measurement of mucosal wave velocity using simultaneous photoglottography and laryngostroboscopy. *Ann. Otol. Rhinol. Laryngol*. 104: 340-349, 1995.
13. Jackson, A.C., Gulesian, P.J. and Mead, J. Glottal aperture during panting with voluntary limitation of tidal volume. *J. Appl. Physiol*. 39: 834-836, 1975.
14. Kouwenhoven, E., Mast, F. and van Rijk-Zwikker, G.L. Geometrical reconstruction of images obtained with electronic endoscopy. *Phys. Med. Biol*. 38: 13-24, 1993.
15. Ma, J.F., Bu, J.J., Hou, K., Bao, S.L. and Chen, C. An energy conduction model for cell image segmentation. *Chinese Sci. Bull*. 56: 1048-1054, 2011.
16. Rattenborg, C. Laryngeal regulation of respiration. *Acta Anaesthesiol. Scand*. 5: 129-140, 1961.
17. Rigau, J., Farre, R., Trepat, X., Shusterman, D. and Navajas, D. Oscillometric assessment of airway obstruction in a mechanical model of vocal cord dysfunction. *J. Biomech*. 37: 37-43, 2004.
18. Smith, W.E., Vakil, N. and Maislin, S.A. Correction of distortion in endoscope images. *IEEE Trans. Med. Imaging* 11: 117-122, 1992.
19. Strauss, R.A. Flexible endoscopic nasopharyngoscopy. *Atlas Oral Maxillofac Surg. Clin. North Am*. 15: 111-128, 2007.
20. Yin, Y.S., Zhao, X.Y., Tian, X.F. and Li, J. Feature-point-extracting-based automatically mosaic for composite microscopic images. *Chinese Sci. Bull*. 52: 1291-1295, 2007.
21. Zhang, Y., Bieging, E., Tsui, H. and Jiang, J.J. Efficient and effective extraction of vocal fold vibratory patterns from high-speed digital imaging. *J. Voice* 24: 21-29, 2004.